Articles

Lateral Assembly of Metal Nanoparticles Directed by Nanodomain Control in Block Copolymer Thin Films

Dehui Yin and Shin Horiuchi*

Nanotechnology Research Institute, National Institute of Advanced Industrial Science and Technology (AIST), 1-1-1, Higashi, Tsukuba, Ibaraki 305-8565, Japan

Toshio Masuoka

Research Institute for Innovation in Sustainable Chemistry, AIST, 1-1-1, Higashi, Tsukuba, Ibaraki 305-8565, Japan

Received August 8, 2004. Revised Manuscript Received October 14, 2004

We have produced and assembled palladium (Pd) nanoparticles in two-dimensional (2-D) periodic arrays in nanoscales by using block copolymer (BC) thin films as templates. A symmetric diblock copolymer of poly(methyl methacrylate)-*block*-poly(2-hydroxyethyl methacrylate) (PMMA-*b*-PHEMA) was coated on a Si-wafer by dip-coating from three different solvents having different solubility against each component. Two of them are selective solvents for PMMA and PHEMA, respectively, and the third one is a common solvent for the two components. A monolayer of the micelles was formed from the solutions of the selective solvents and the micelles are arranged in a hexagonal 2-D lattice, whereas a lamellar pattern was obtained from a homogeneous solution of the common solvent. The monolayer films thus-prepared were exposed to the vapor of palladium (II) bis(acetylacetonato), and Pd nanoparticles were selectively produced in the PHEMA phase due to its stronger reducing power than the PMMA phase. The patterns thus-obtained were successfully transferred to a Si-wafer by reactive dry etching technique because of the high etching resistivity of the metal nanoparticles against gas plasmas. By using this process, three lateral periodic arrays of dots, holes, and lines were created with 20-nm repeating distances.

Introduction

Syntheses, patternings, and applications of metal nanoparticles have been extensively investigated because of their potential for building blocks for nanodevices.[1−6] It is well-known that metal nanoparticles possess unique properties associated with magnetic, photonic, chemical, and electric behaviors, which are different from the properties in their bulk states. Those properties can be controlled through the immobilization and the assembly of nanoparticles on an appropriate substrate or in a suitable medium. The patternings of metal nanoparticles over a wide range of scales and dimensions have been recognized as a key technology for constructing nanoscale magnetic, electric, and chemical systems.

We have developed a simple dry process for synthesis and assembling of metal nanoparticles in polymer films through the reduction of a metal complex used as a precursor.[4−7] Palladium(II) bis(acetylacetonato), denoted $Pd(acac)_2$, is vaporized in ambient nitrogen at atmospheric pressure at 180 °C, and is exposed to a polymer film in a glass vessel for a period of 15 min to 2 h depending on the reducing behavior of the polymers employed. The vapor can penetrate into a polymer film and is simultaneously reduced to form Pd metallic particles with diameters ranging from 2 to 10 nm with narrow size distributions. Cobalt nanoparticles also can be synthesized using the corresponding metal complex by the same procedure.[6] For the production of metal nanoparticles in this process, no catalyst is required for the reduction of the metal complex, which means that polymer films themselves have the catalytic activity to reduce the metal complex. As reported in our previous papers,[5,6] the absorption and reduction behaviors of polymers are different from each other. The detailed mechanism of the process, however, remains unknown at this point. The diblock copolymer films with a proper combination of polymers having different reducing powers produce nanoscale assembly of metal

* Corresponding author. E-mail: s.horiuchi@aist.go.jp. Tel: +81-3-3588-8309. Fax: +81-3-3599-8166.

(1) Fendler, J. H., Ed.; *Nanoparticles and Nanostructured Films: Preparation, Characterization and Applications*; Wiley-VCH: Weinheim, 1998.
(2) Rotello, V., Ed.; *Nanoparticles: Building Blocks for Nanotechnology*; Kluwer Academic/Plenum Publishers: New York, 2004.
(3) Heilmann, A. *Polymer Films with Embedded Metal Nanoparticles*; Springer-Verlag: New York, 2003.
(4) Nakao, Y. *Chem. Lett.* **2000**, 766−767.
(5) Horiuchi, S.; Sarwar, M. I.; Nakao, Y. *Adv. Mater.* **2000**, *12*, 1507−1511.
(6) Horiuchi, S.; Fujita, T.; Hayakawa, T.; Nakao, Y. *Langmuir* **2003**, *7*, 2963−2973.
(7) Horiuchi, S.; Fujita, T.; Hayakawa, T.; Nakao, Y. *Adv. Mater.* **2003**, *15*, 1449−1452.

10.1021/cm048695g CCC: $30.25
Published on Web 01/11/2005

nanoparticles due to the selective growth of the metal nanoparticles in the phase with relatively stronger reducing power. The vapor of the metal complex can penetrate into a polymer film, and the patterns thus-obtained reflect the microdomain structures of the block copolymers (BCs). Therefore, this process gives rise to the formation of three-dimensional (3-D) regular assembly of metal nanoparticles with the depth of about 100 μm.

In addition to this nanoscale ordered assembly of metal nanoparticles, we have also reported on the capability of arbitrary microscale patterning of metal nanoparticles by UV lithography.[7] We found that the irradiation of UV light on poly(methyl methacrylate) (PMMA) enhances its reducing power against $Pd(acac)_2$. Therefore, irradiation through a photomask on a PMMA film can produce arbitrary patterns of the aggregation of metal nanoparticles.

For the investigation of the practical applications of the polymer/metal nanoparticles systems prepared by our method, we have already reported on the catalyst properties of the Pd nanoparticles that enable electroless deposition of metals and metal oxides on a substrate.[8] For the development of industrial applications, the construction of two-dimensional (2-D) nanoscale assembly of metal nanoparticles in a BC thin film coated on a substrate has to be developed. Self-assembled BCs have been frequently employed as templates for works in the area of nanolithography, high-density storage media, and photonic devices.[9,10] In this current work, we have investigated the formation of the nanodomain structures in amphiphilic BC monolayer films and the selective incorporation of the Pd nanoparticles into a phase to prepare laterally ordered assembly of metal nanoparticles. Moreover, we have evaluated the pattern transfer to underlying Si-wafers by reactive ion etching (RIE) by employing the BC/metal nanoparticle systems as lithography masks.

Experimental Section

Materials. $Pd(acac)_2$ was purchased from Johnson Matthey Materials Technology and was recrystallized from acetone before use. The symmetric diblock copolymer of poly(methyl methacrylate)-*block*-poly(2-hydroxyethyl methacrylate) (PMMA-*b*-PHEMA, M_n = 24 300/16 700) was used as received from Polymer Source Inc. Pyridine, 1,4-dioxane, methanol, and 2-methoxyethanol (2-MOE) were purchased from Wako Pure Chemical Industries, Ltd. and used as received.

Preparation of Films. The free-standing film of PMMA-*b*-PHEMA was prepared by casting from 2 wt % pyridine solution. The solution was dried at 50 °C on a hot plate for 1 day at atmospheric pressure, and then dried in a vacuum oven at 200 °C for 12 h followed by annealing at 150 °C for 24 h. Thin films of PMMA-*b*-PHEMA were made on Si-wafers with a native oxide layer or on a carbon thin film supported by a copper grid for electron microscopy. All these films were made by dip-coating using homemade equipment. The substrates were dipped into the 0.5 wt % solution of 1,4-dioxane, methanol, or 2-methoxyethanol with a velocity of 40 mm/min, subsequently pulled out of the solution with a velocity of 5 mm/min, and then exposed to air for drying. The Si-wafers were rinsed by acetone and then treated by oxygen plasma at 10 W for 10 min at gas pressure of 20 Pa before use.

Incorporation of Pd Particles into the Films. The process developed by our group[5−7] was employed to incorporate Pd nanoparticles selectively into the PHEMA phase of the PMMA-*b*-PHEMA film. The bottom of a glass vessel with 10 mg of $Pd(acac)_2$ was heated at 180 °C in vacuo to sublime the $Pd(acac)_2$, and then within a few minutes the $Pd(acac)_2$ was solidified on the upper part of the glass wall. In the next step, a BC film was loaded into the glass vessel, and the sealed glass vessel was put into an oil bath at 180 °C for 30 min after nitrogen replacement.

Plasma Etching. The substrates coated with a BC thin film were treated with a gas plasma using an in-house fabricated tubular reactor which generates capacitively coupled plasma excited by a 13.56-MHz RF power source. In the case of oxygen plasma, the samples were treated at 90 W for 30 min at gas pressure of 0.5 Torr. In the case of CF_4 plasma, the samples were treated at 1 W for 30 min at gas pressure of 0.08 Torr.

Characterization. Transmission electron microscopy (TEM) micrographs were acquired with a LEO922 energy-filtering transmission electron microscope (LEO Eletronenmikroskopie GmbH, Germany) at an accelerating voltage of 200 kV, which integrates an Omega-type electron spectrometer. Zero-loss images and energy-filtered images were acquired with an energy width of 20 eV. For the cross-sectional view by TEM, the films embedded in resin were cut by means of ultramicrotomy with a diamond knife. Scanning force microscopy (SFM) images were taken with a SPA 300HV (Seiko Instruments Inc., Japan) in the tapping mode. To achieve high-quality images, a cantilever with a super-sharp tip (SI-DF20S, Seiko Instruments Inc., Japan, spring constant of 20 N/m and radius of curvature <2−3 nm) was used. Scanning electron microscopy (SEM) images were taken with a Philips XL30 FE-SEM at an acceleration voltage of 10 kV. Statistical image analysis was performed using a digital image analysis software (analySIS, Soft Imaging System Co. Ltd., Germany). The thickness of thin films was measured by a JASCO M-220 spectroscopic ellipsometer.

Results and Discussion

Nanodomain Control of PMMA-*b*-PHEMA Thin Films by Dip Coating. We have evaluated the reduction of $Pd(acac)_2$ and the formation of Pd nanoparticles in various homopolymer films.[5,6] During our studies we learned a unique behavior of PMMA with respect to the absorption and reduction of metal complex. We found that all the evaluated polymers but PMMA absorb and reduce the metal complex simultaneously. In the case of PMMA, although it also absorbs metal complex vapor like the other polymers do, it tends to retard the reduction and the formation of nanoparticles. We also learned that polymers having alcoholic hydroxyl moieties exhibit strong reducing power. Thus, it can be predicted that a BC composed of PMMA and a polymer with an alcoholic moiety will exhibit significant difference in their reducing power, and will yield distinct patterns of nanoparticles. Figure 1 shows a cross-section of the free-standing PMMA-*b*-PHEMA symmetric diblock copolymer film exposed to $Pd(acac)_2$ vapor for 30 min. It clearly exhibits a 3-D pattern by Pd nanoparticles' assembly with a periodic lamellar manner, which reasonably corresponds to the underlying nanodomain structure of the symmetric diblock copolymer. As we reported in the previous paper,[5,6] longer periods of up to 2 h were required to achieve such a distinct pattern in polystyrene-*block*-poly(methyl

(8) Lee, J. Y.; Yin, D.; Horiuchi, S. to be submitted for publication.
(9) Wang, X.; Liu, Y.; Zhu, D. *Adv. Mater.* **2002**, *14*, 165−167.
(10) Lazzari, M.; López-Quintela, M. A. *Adv. Mater.* **2003**, *15*, 1583−1594.

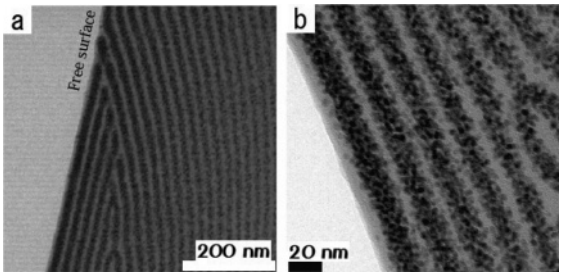

Figure 1. TEM micrographs of a cross section of a PMMA-*b*-PHEMA free-standing film exposed to $Pd(acac)_2$ vapor for 30 min; and (b) magnified image showing the region just below the free surface of the film.

methacrylate) (PS-*b*-PMMA), where Pd metal nanoparticles were assembled in the PS lamellae. The formation of the pattern by the Pd nanoparticles in PMMA-*b*-PHEMA in such a short time is attributed to the strong reducing power of the PHEMA component.

It has been well-known that the free surface of BC film tends to cover itself with a component having relatively low surface tension to minimize the surface energy.[11] This induces the parallel orientation of several lamellae from the outermost surface. The higher magnification micrograph (Figure 1b) focused on the free surface of the film shows that the Pd metal nanoparticles are located in the second layer of the film from the free surface, suggesting that the PMMA phase predominantly is located at the air/polymer surface. This tendency is the same as that of polystyrene-*block*-PHEMA films.[12]

To realize the 2-D regular assembly of the metal nanoparticles, PMMA-*b*-PHEMA monolayer films possessing laterally ordered nanodomains over entire films have to be prepared on substrates. The conventional spin-coating from a dilute solution yields no regular patterns of nanoscopic domains in a thin film. Thus, many efforts have been made to control the orientation or the lateral ordering of the nanoscopic domains of BCs, using external fields, such as electric fields,[13,14] shear[15,16] and temperature gradients,[17] micelle formation in a selective solvent,[18] and solvent evaporation.[19] In this work, we have realized three distinct regular patterns using one BC by dip-coating from three different solvents.

PMMA-*b*-PHEMA is an amphiphilic block copolymer, hence treating the polymer with a selective solvent, which dissolves one component and does not dissolve the other, yields a micellar solution. Three solvents, 1,4-dioxane, methanol, and 2-MOE, were chosen for the film preparation by dip-coating. 1,4-Dioxane is a selective solvent for the PMMA component, methanol is a selective solvent for PHEMA, and 2-MOE is a common solvent for both components. Therefore, the BC micelles with the PHEMA cores and the PMMA shells are formed in 1,4-dioxane, and the inverted micelles are obtained in methanol. By pulling the substrates out of the 0.5 wt % solutions with a velocity of 5 mm/min, the monolayer films with distinct regular patterns can be achieved instantly as shown by SFM images in Figure 2. Figure 2 shows the topography images of the surface structures of the as-cast films dip-coated from the three solutions on Si-wafers. The films prepared from the 1,4-dioxane solution (Figure 2a) and from the methanol solution (Figure 2b) show that the spheres are arranged in a 2-D hexagonal lattice, while the film from the 2-MOE solution shows a stripe pattern (Figure 2c) which is typical in a thin film of a symmetric diblock copolymer. The thickness of the films was about 20 nm, as measured by an ellipsometer, indicating that the films are nearly monolayers.

Quantitative image analysis suggests the difference in the structure of the films coated from the two micellar solutions. The film coated from the 1,4-dioxane solution possesses spheres with average diameter of 24 nm and average distance between neighboring spheres of 35 nm, while the film from the methanol solution possesses spheres with average diameter of 30 nm and the particles seem to be closely packed. The profiles shown at the bottom of the individual images are the height variations along the lines shown in the corresponding images. The height variation between the elevated domains and the matrix are in the range from 2 to 3 nm in the film from the 1,4-dioxane solution, while the film coated from the methanol solution exhibits a little larger degree of the variations. Considering those facts, we can speculate the structure of the films coated from the 1,4-dioxane solution and from the methanol solution as shown in Figure 3. In the film dip-coated from the 1,4-dioxane solution, the micelles are collapsed to form a dense melt-like film, where the elevated PHEMA domains are arranged in a continuous PMMA matrix. On the other hand, the film coated from the methanol micellar solution shows the simple array of the micelles with the PMMA cores surrounded by PHEMA. Another difference that we can identify from the two films is that the space between the neighboring domains is a little larger in the film coated from 1,4-dioxane. This may be caused by the formation of the continuous film during the coating. We suspect that these differences in the film formation are caused by the difference in the adsorption behavior of the micelles on a Si-wafer derived from the difference in the preferences of the two components for the substrate.

From the illustration in Figure 3b, the height variation along two neighboring particles in the SFM topographic image should be equal to the radius of the particles (15 nm). However, experimental data (ca. 6 nm) indicate it is less than half of this value. The reason for this discrepancy is that the tip size of the cantilever is significantly larger than the narrow space between the neighboring particles. This may cause the broadening of the boundary. Therefore, it would

(11) Russell, T. P.; Coulon, G.; Deline, V. R.; Miller, D. C. *Macromolecules* **1989**, *22*, 4600−4606.
(12) Senshu, K.; Yamashita, S.; Ito, M.; Hirao, A.; Nakahama, S. *Langmuir* **1995**, *11*, 2293−2300.
(13) Morkved, T. L.; Lu, M.; Urbas, A. M.; Ehrichs, E. E.; Jaeger, H. M.; Mansky, P.; Russell, T. P. *Science* **1996**, *273*, 931−933.
(14) Thurn-Albrecht, T.; DeRouchey, J.; Russell, T. P.; Jaeger, H. M. *Macromolecules* **2000**, *33*, 3250−3253.
(15) Albalak, R. J.; Thomas, E. L.; Capel, M. S. *Polymer* **1997**, *38*, 3819−3825.
(16) Villar, M. A.; Rueda, D. R.; Ania, F.; Thomas, E. L. *Polymer* **2002**, *43*, 5139−5145.
(17) Bodycomb, J.; Funaki, Y.; Kimishima, K.; Hashimoto, T. *Macromolecules* **1999**, *32*, 2075−2077.
(18) Spatz, J. P.; Mössmer, S.; Hartmann, C.; Möller, M.; Herzog, T.; Krieger, M.; Boyen, H.-G.; Ziemann, P.; Kabius, B. *Langmuir* **2000**, *16*, 407−415.
(19) Kim, S. H.; Misner, M. J.; Xu, T.; Kimura, M.; Russell, T. P. *Adv. Mater.* **2004**, *16*, 226−231.

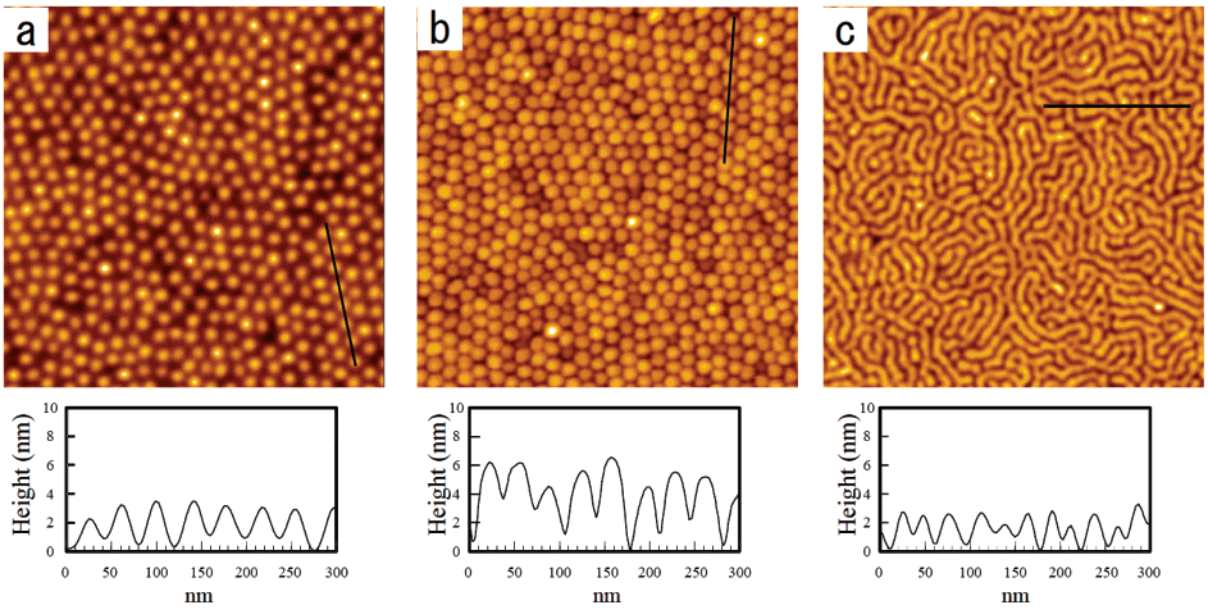

Figure 2. SFM topography images of PMMA-*b*-PHEMA thin films dip-coated from 0.5 wt % solutions of three different solvents: (a) 1, 4-dioxane; (b) methanol; and (c) 2-methoxy ethanol. The length of each image corresponds to 800 nm. The profiles shown at the bottom of the images are the height variations along the lines indicated in the corresponding images.

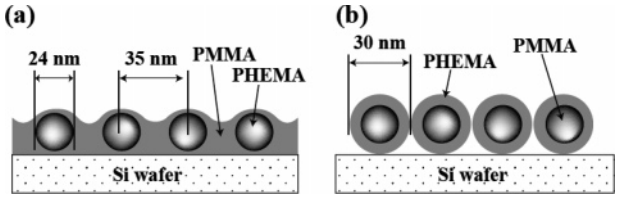

Figure 3. Schematic drawing of the side views of thin films of PMMA-*b*-PHEMA adsorbed onto a Si-wafer dip-coated from (a) 1, 4-dioxane and (b) methanol micellar solutions.

be safe to assume that the qualitative picture of the surface roughness would be more valuable than the quantitative accuracy of the height profiles obtained from such measurements.

Lateral Ordered Assembly of Pd Nanoparticles in Block Copolymer Thin Films. Using the three patterns obtained from PMMA-*b*-PHEMA thin films by dip-coating as templates, Pd nanoparticles can be laterally assembled by the exposure of the $Pd(acac)_2$ vapor for 30 min in ambient nitrogen at atmospheric pressure at 180 °C. Figure 4 shows the SFM topography images and TEM micrographs of the thin films after incorporation of the Pd nanoparticles. The SFM images (Figure 4a−c) were obtained from the films coated on Si-wafers and the TEM micrographs (Figure 4d−i) were taken from the films coated on carbon thin films with TEM copper grids. The Pd nanoparticles are selectively located in the PHEMA phase; hence, the three assembly patterns of the Pd nanoparticles reflecting the underlying nanodomain structures can be obtained as shown in the TEM micrographs. Figure 4g−i are high magnification views of Figure 4d−f, respectively, presenting that the Pd nanoparticles with diameters of about 3 nm are assembled in the spherical domains, in the matrix, and in the lamellae formed by the PHEMA component, respectively. The low magnification view of the film dip-coated from 1,4-dioxane (Figure 4d) is shown by an electron energy-loss image at 250±10 eV losses to enhance the contrast, where an element with a higher atomic number appears as brighter regions.[20] This clearly indicates that the Pd nanoparticles are assembled in the PHEMA domains ordered in a 2-D hexagonal lattice. The inset in Figure 4d is the fast Fourier transform (FFT) calculated from this image, indicating the long-range hexagonal order of the domains with the lattice spacing of 39 nm. Although the SFM image (Figure 4a) shows all the domains as isolated spheres, some domains seem to be coalesced, and the hexagonal lattice order seems to be disordered in the TEM image (Figure 4d). One of the reasons is thought to be the specimen damage caused by the electron beam during the TEM observation. The electron beam causes damage against polymers, and PMMA especially can be easily degraded even with relatively low doses.[21] The other reason is the instability of the carbon thin film used for a substrate. The carbon thin film cannot fix the BC thin films sufficiently as compared to a Si-wafer, and hence in the process of incorporation of Pd nanoparticles, the BC tends to be changed into the thermodynamically stable lamellar pattern. This phenomenon was also observed in the film dip-coated from the methanol micellar solution. As presented in Figure 4e and h, the PHEMA continuous matrix with the Pd nanoparticles is partially collapsed and disordered. Since the corresponding SFM image shows no such phenomena, it is inferred that this is also caused by the instability of the substrate and the electron beam damage.

As can be seen in the SFM images (Figure 4a−c), the laterally ordered nanodomain structures obtained by dip-coating are maintained in all the three films after the process to incorporate the Pd nanoparticles. However, one can recognize that the surface topographic feature of the film prepared from the methanol solution (Figure 4b) is changed from that of the as-cast film (Figure 2b), where the domains appear as darker regions with the average diameter of 25

(20) Reimer, L. In *Energy-Filtering Transmission Electron Microscopy*; Reimer, L., Ed.; Springer: Münster, 1995; Chapter 7, p 347.
(21) Hiraoka, H. *IBM J. Res. Dev.* **1977**, 121−130.

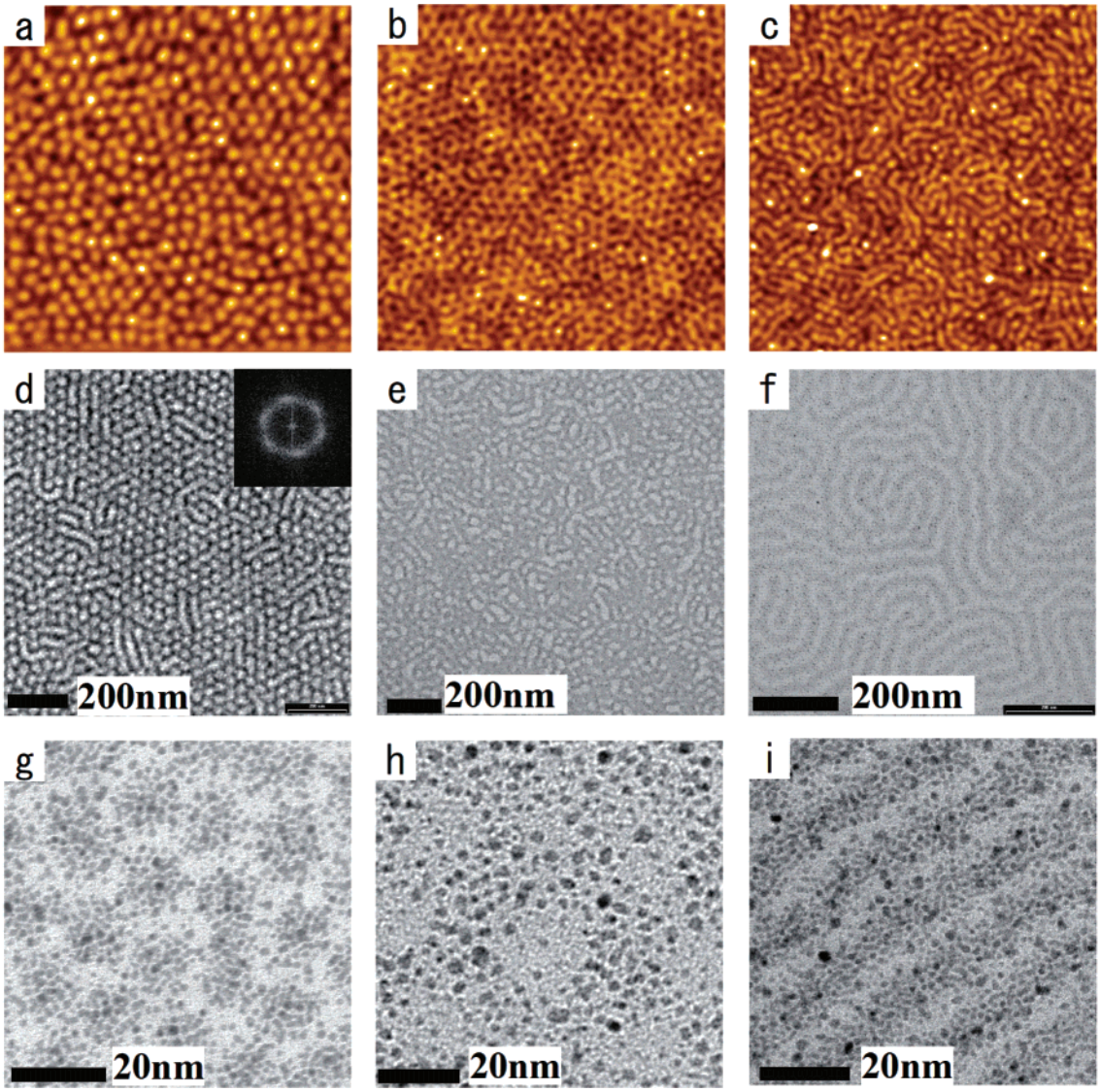

Figure 4. SFM topography images (a−c) and TEM micrographs (d−i) of PMMA-*b*-PHEMA thin films exposed to $Pd(acac)_2$ vapor for 30 min. Left column is the film prepared from 1,4-dioxane micellar solution, center column is from methanol micellar solution, and right column is from 2-methoxy ethanol homogeneous solution. (d) Energy-filtered image at 250±10 eV energy losses on EFTEM to give a proper contrast between the matrix and the domains. Inset of (d) is a FFT power spectrum of the image. (g−i) Bright field images of (d−f), respectively, at higher magnifications to show the individual Pd nanoparticles selectively located in the PHEMA phase. The length of each SFM image corresponds to 800 nm.

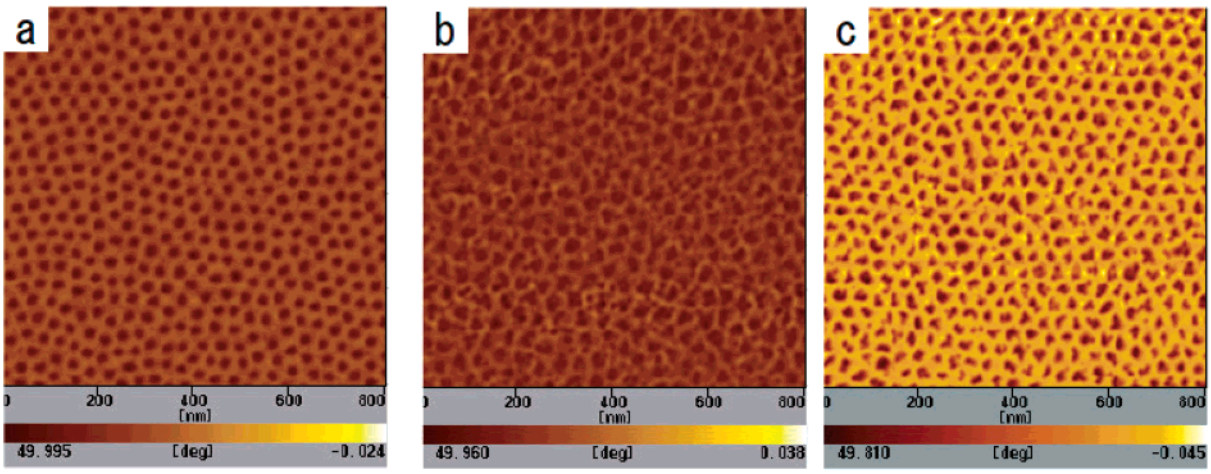

Figure 5. SFM phase shift images of PMMA-*b*-PHEMA thin films dip-coated from 1,4-dioxane solution at different processing steps for pattern transfer onto a Si-wafer by RIE: (a) as-cast film; (b) after loading of Pd nanoparticles by the exposure of $Pd(acac)_2$ vapor for 30 min; and (c) after oxygen plasma treatment. All the images are shown in the range of the phase shift from 0 to 50 degrees. The length of each image corresponds to 800 nm.

nm. It can be interpreted that the hexagonally arranged micelles are melted to form a continuous matrix because the film is laid at 180 °C during the exposure to the $Pd(acac)_2$ vapor. And also, the Pd particles are selectively incorporated into the PHEMA matrix as shown in Figure 4e and h, which causes an increase in the volume of the PHEMA phase. Therefore, the PHEMA phase exhibits the elevated continuous matrix with the PMMA domains in the SFM topography image.

Pattern Transfer onto Si-Wafers by Reactive Ion Etching. Self-organizing BCs used for lithography masks under conventional RIE are expected to create small features on substrates that cannot be achieved by standard lithography techniques.[22−27] The loading of metal species selectively into a phase in BC thin films is one of the approaches to enhance the etching selectivity against RIE. Therefore, we evaluated our technique as nanolithography masks as one of the expected applications.

In the first step, O_2 plasma was applied to BC thin films with the Pd nanoparticles for selective removal of the polymer. The phase-shift images clearly exhibit changes in the surface stiffness features as shown in Figure 5. Figure 5a−c are the phase shift images of the as-cast film prepared by dip-coating from the 1,4-dioxane micellar solution, after the loading of Pd nanoparticles into the film, and after the O_2 plasma treatment, respectively; all of which are displayed in the same range of the degree of phase shift (from 0 to 50 degrees). The series of images indicates that the surface component is significantly changed at every step in the process. That is, the image contrast decreases after loading of Pd nanoparticles into the PHEMA domains (Figure 5b), and then it increases again after the O_2 plasma treatment (Figure 5c) where the contrast is offered by the difference in the surface features between the assembled Pd nanoparticles and the naked Si-wafer. We also confirmed the existence of Pd nanoparticles after the O_2 plasma treatment by X-ray photoelectron spectroscopy. This measurement also revealed that the characteristic peak of Pd $3d_{5/2}$ is shifted from 340 to 344 eV after the O_2 plasma treatment, which suggests that the Pd nanoparticles are converted to Pd oxides. The statistical image analysis of Figure 5c reveals that the average domain size is 22 nm and the mean center-to-center distance between the closest particles is 34 nm. Therefore, it has been confirmed that the O_2 plasma allows the removal of the polymer while maintaining the patterns that the BC thin films initially possess throughout the process.

In the next step, the O_2 etched films were treated by CF_4 plasma. The region under the Pd nanoparticles on the Si-wafer is masked against the CF_4 plasma, thus the naked Si-wafer is etched at a higher rate and the nanodomain patterns of the BC thin films can be transferred to Si-wafers. Figure 6 shows the SEM micrographs of the three patterns produced on Si-wafers by using the BC thin films with the periodically assembled Pd nanoparticles presented in Figure 4 as lithography masks. Those micrographs qualitatively present that the substrates are etched by the CF_4 plasma treatment because the patterns before the CF_4 plasma treatment cannot be seen

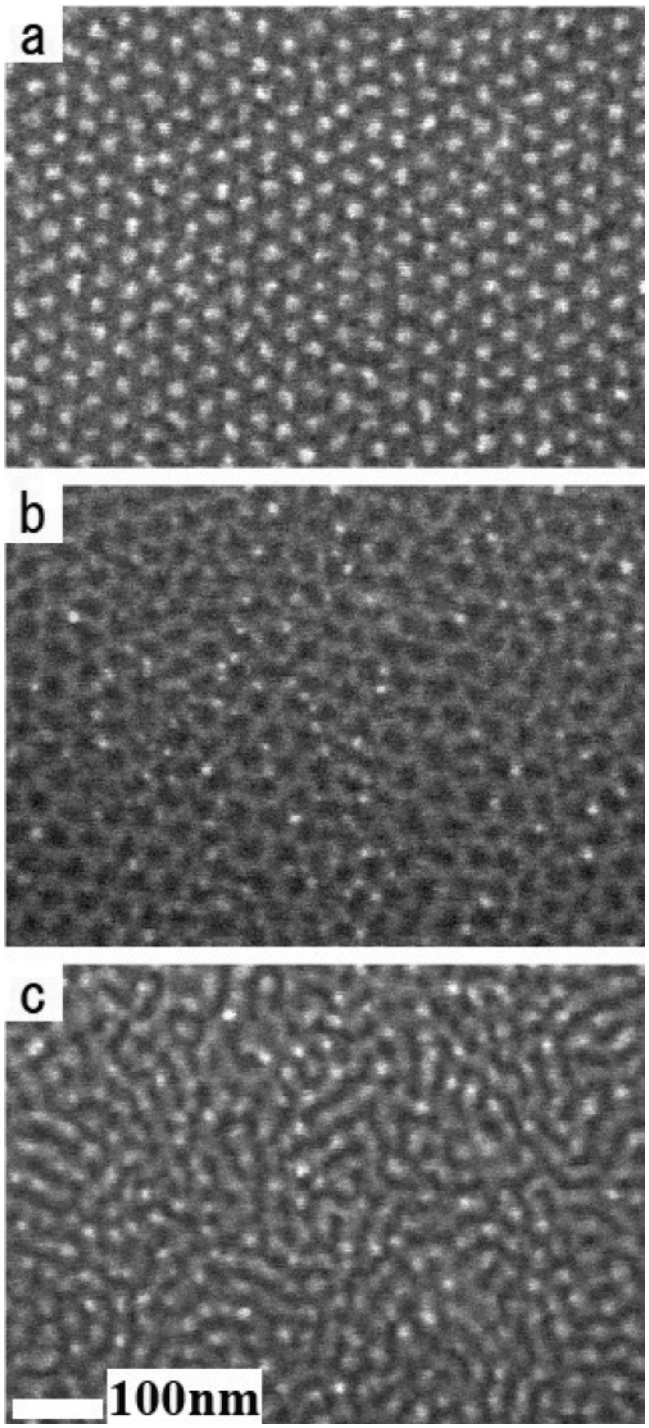

Figure 6. SEM micrographs of the three patterns transferred onto Si-wafers by RIE using PMMA-*b*-PHEMA thin films with Pd nanoparticles as lithography masks; (a−c) were produced by using the PMMA-*b*-PHEMA films dip-coated from 1,4-dioxane, methanol, and 2-methoxy ethanol solutions, respectively.

(22) Park, M.; Harrison, C.; Chaikin, P. M.; Register, R. A.; Adamson, D. H. *Science* **1997**, *276*, 1401−1404.
(23) Park, M.; Chaikin, P. M.; Register, R. A.; Adamson, D. H. *Appl. Phys. Lett.* **2001**, *79*, 257−259.
(24) Spatz, J. P.; Eibeck, P.; Mössmer, S.; Möller, M.; Herzog, T.; Ziemann, P. *Adv. Mater.* **1998**, *10*, 849−852.
(25) Lammertink, R. G. H.; Hempenius, M. A.; van den Enk, J. E.; Chan, V. Z.-H.; Thomas, E. L.; Vancso, G. J. *Adv. Mater.* **2000**, *12*, 98−103.
(26) Cheng, J. Y.; Ross, C. A.; Chan, V. Z.-H.; Thomas, E. L.; Lammertink, R. G. H.; Vancso, G. J. *Adv. Mater.* **2001**, *13*, 1174−1178.
(27) Naito, K.; Hieda, H.; Sakurai, M.; Kamata, Y.; Asakawa, K. *IEEE Trans. Magn.* **2002**, *38*, 1949−1951.

clearly by SEM. This means that three different periodic patterns, where the feature sizes and the half pitches are as small as 20 nm, can be produced on Si-wafers using one BC.

Conclusions

The assemblies of Pd nanoparticles with the three different lateral patterns can be achieved on Si-wafers by using BC thin films as templates. We showed that the nanodomain patterns of the PMMA-*b*-PHEMA monolayer film can be controlled by dip-coating in appropriate selection of solvents. The patterns with lateral periodicities of the BC thin films on Si-wafers prepared by dip-coating can be maintained throughout the process for the incorporation of the Pd nanoparticles using the $Pd(acac)_2$ vapor as a precursor even though the films was laid at 180 °C for 30 min. The advantage of our technique is that the three different 2-D patterns can be achieved using one BC with a relatively simple dip-coating technique that requires no further procedures to gain the orientation or ordering of the domains in BC films; also, the metal nanoparticles can be loaded into the films by a simple dry process while maintaining the lateral orders of the films.

As one of the applications of our technique, the pattern transfer of the assemblies of the Pd nanoparticles onto Si-wafers was successfully carried out. Loading of the Pd nanoparticles selectively into a phase of the BC thin films can enhance the etching selectivity against RIE, which enables the creation of the periodic patterns with small feature sizes that cannot be achieved by standard lithography techniques. Thus, the hexagonal arrays of dots and holes can be produced on Si-wafers by using the BC thin films dip-coated from the micellar solutions, and also the lamellar pattern can be produced from the homogeneous solution. Patterns of complex geometries need to be created for integrated circuits, while some technological applications, including the fabrication of densely packed magnetic domains[27,28] or silicon capacitors with increased charge storage capacity,[29] require only a regular array of domains on substrates. Our technique can provide the lithography masks by a simple and practical easy process with an amphiphilic diblock copolymer that can be synthesized without complex schemes.

In addition, patterning the Pd nanoparticles will provide catalyst surfaces that enable the growth of functional materials, such as metals, semiconductors, ceramics, and carbon nanotubes, on a surface in a controllable fashion, which possesses potential application for nanoelectronics, flat-panel displays, sensors, and so on.[30−33] We will continue the investigation of the possibility of our technique for various applications.

Acknowledgment. Financial support by New Energy and Industrial Technology Development (NEDO) for the Nanostructured Polymer Project is gratefully acknowledged.

CM048695G

(28) Thurn-Albrecht, T.; Schotter, J.; Kästle, G. A.; Emley, N.; Shibauchi, T.; Krusin-Elbaum, L.; Guarini, K.; Black, C. T.; Tuominen, M. T.; Russell, T. P. *Science* **2000**, *290*, 2126−2129.
(29) Black, C. T.; Guarini, K. W.; Milkove, K. R.; Baker, S. M.; Russell, T. P.; Tuominen, M. T. *Appl. Phys. Lett.* **2001**, *79*, 409−411.
(30) Huang, S.; Dai, L.; Mau, A. W. H. *Adv. Mater.* **2002**, *14*, 1140−1143.
(31) Saito, N.; Haneda, H.; Sekiguchi, T.; Ohashi, N.; Sakaguchi, I.; Koumoto, K. *Adv. Mater.* **2002**, *14*, 418−421.
(32) Chen, M. S.; Brandow, S. L.; Dressick, W. J. *Thin Solid Films* **2000**, *379*, 203−212.
(33) Ma, D. I.; Shirey, L.; McCarthy, D.; Thompson, A.; Qadri, S. B.; Dressick, W. J.; Chen, M. S.; Calvert, J. M.; Kapur, R.; Brandow, S. L. *Chem. Mater.* **2002**, *14*, 4586−4594.